Supplementary Material and Methods

Chromatin Immunoprecipitation
Three micrograms of antibody was prebound for 8h to protein A and protein G Dynal magnetic beads (Dynal Biotech, Norway) and washed 5x with ice-cold PBS containing 5% BSA, and then added to the diluted chromatin for overnight immunoprecipitation using the following antibodies: TCF-4 (Upstate #05-511), mouse IgG2a isotype control (Sigma, M5409), and rabbit IgG (sc-2027, Santa Cruz). The magnetic bead-chromatin complexes were collected and washed 6x in RIPA buffer (50 mM HEPES [pH 7.6], 1 mM EDTA, 0.7% Na-deoxycholate, 1% NP-40, 0.5 M LiCl). DNA was eluted from the beads as previously described(54). Amplification was carried out with a PTC-200 programmable thermal controller (MJ Research) after an initial denaturation at 94°C for 5min, followed by 30 cycles of PCR using the following temperature and time profile: denaturation at 94°C for 0.5min, primer annealing at 59°C for 0.5min, primer extension at 72°C for 0.5min, and a final extension of 72°C for 10min. The PCR products were visualized by 2% gel electrophoresis. The following promoter primer sets were employed: (1) *VEGF* (*55*): gcgtgtctctggacagag-ttt; agcctcagcccttccaca; (2) *VEGF* upstream: gaggctatgccagctgtagg; ccctt-ttcctccaactctcc; (3) *c-MYC*:actcccccggctcggtccacaagc; cccaatttctcagccaggtttcag.

Patient Specimens and Cell Lines
Bone marrow specimens were obtained from patients with MM in accordance with Dana-Farber Cancer Institute Review Board approval and informed consent performed in compliance with the Declaration of Helsinki. Primary CD138+ plasma cells were purified using magnetic beads as described (*16*). CRC primary tumor samples were obtained from the Brigham and Women's Hospital in accordance with the policies of their Institutional Review Board. To generate sufficient CRC primary tumor cells for experimentation, the primary tumors were first expanded subcutaneously in NOD/SCID mice (Jackson Laboratory). After the tumors reached 2cm in diameter, mice were sacrificed according to institutional guidelines and subcutaneous tumor xenografts were minced with a scalpel and digested by incubation with collagenase IV (Worthington Biomedical Corporation) and 0.01% DNase I (Sigma-Aldrich) at 37°C for 30min, followed by additional mechanical disaggregation using a Stomacher device (Seward Laboratory Systems Inc.). Samples were filtered through a 70μm cell strainer and washed with PBS. Red blood cells were lysed using ACK lysing buffer (BioWhittaker, Lonza) and viable tumor cells were enriched by Ficoll-Paque gradient centrifugation (GE Healthcare). To purify viable tumor cells only, the samples were treated with APC conjugated anti-mouse H-2Kd (clone SF1-1.1.1, eBioscience), FITC-conjugated anti-human EpCAM antibodies (clone Ber-EP4, Dako), and Hoechst 33258 (Sigma-Aldrich), and then FACSAria flow sorting (BD Biosciences) was used to isolate the EpCAM-positive, H-2Kd-negative, and Hoechst-negative primary tumor cells. Cultured cell lines were maintained as previously described(19).

Quantitative Reverse Transcription-PCR

RNA was extracted with TRIzol Reagent (Invitrogen) according to the manufacturer's protocol. Total RNA (2 µg) was reverse transcribed (SuperScript VILO cDNA synthesis kit, Invitrogen) and qPCR was performed using an Applied Biosynthesis 7500 Real-time PCR system. Analysis of target genes was conducted in quadruplicate using POWER SYBR Green Master Mix (Applied Biosystems) as previously described(19). Transcripts levels were normalized to β-actin expression. These experiments were repeated three times. PCR primers are designed as below:

FOXQ1: cgcggactttgcactttgaa; agctttaaggcacgtttgatggag. *CDK4*: atgttgtccggctgat -gga; caccagggttaccttgatctcc. Axin2: cggaaactgttgacagtggat; ggtgcaaagacatagcc -agaa. *VEGF*: catgaactttctgctgtcttgg; atgattctgccctcctcctt. *LGR5*: ctcccaggtctggtgt -gttg; gtgaagacgctgaggttgga. *CMYC*: tttttcggggtagtggaaaacc; gcagtagaaatacggctg-cac. *CD44*: tttgcattgcagtcaacagtc; tgagtccacttggctttctgt. *CLDN2*: cggtgtggctaagta -caggc; caaagctcacgatggtggtct. *LEF-1*: catcccttcctcattccttcaac; aggcttcctaaaaggt -ggtgg.

Establishment of Single Cell Cultures

Colo320 cells were subjected to infection for 72h with either 7xTdG or 7xFdG lentivirus, and the transduced and control non-transduced cells were trypsinized, washed, and then analyzed on a FACSaria flow sorter. Hoechst 33258 staining was used to exclude dead cells. Single GFP-positive Colo320-7xTdG cells were sorted into 96 well plates using stringent gating on forward/side scatter height and width to exclude doublets. The presence of a single cell per well was confirmed microscopically after sorting and then single cell cultures were expanded for subsequent use.

Fluorescence Microscopy

Cells were prepared using a cytocentrifuge (Thermo Shandon) and fixed as previously described(16, 19). Anti-β-catenin and rhodamine-conjugated secondary antibodies (5µg/ml; Southern Biotechnology) were employed. Images were obtained using a BioRad Radiance 2000 laser and Leica TCS SP5 scanning confocal microscopy.

Lentiviral Vectors

A lentiviral reporter vector containing seven TCF/LEF-1 binding motifs and a minimal promoter driving destabilized GFP expression (7xTdG) was derived from the lentiviral vector TOP-dGFP, which contains three TCF/LEF-1 binding motifs(45). Two synthetic complementary oligonucleotides (IDT-DNA) with four TCF/LEF-1 binding motifs (GATCAAAGG) were designed to generate compatible overhanging ends for annealing to an *Xba*1 restriction site. The oligonucleotides were annealed by heating to 95°C and slow cooling to room temperature, followed by ligating into the *Xba*1-linearized TOP-dGFP vector, yielding 7xTdG. For construction of the control vector carrying seven FOP-sites (7xFdG), the 7xTOP cassette was removed from the 7xTdG vector by restriction digesting with *Xma*1 and *Age*1. A synthetic cassette carrying seven FOP sites (GGCCAAGG)

but otherwise identical to the removed 7xTOP cassette was inserted, yielding 7xFdG. BCL9 shRNA and control shRNA lentiviral vectors were generated as reported(56).

Lentivirus Production and Infection

HEK293T cells were plated in 10cm tissue culture dishes and co-transfected with 10μg lentiviral vector (either 7xTdG or 7xFdG), 10μg pCMV-dR8.91 and 2μg pMD2.G (57) using 60μL LipoD293 (Signagen) according to the manufacturer's protocol. The media was replaced after 12h with 30% FCS containing DMEM (Gibco) and conditioned for 36h. Conditioned medium was then filtered through 0.45μm syringe filters (Millipore), mixed 1:1 with fresh DMEM, and then directly used for infection of cultured Colo320 (ATCC) cells. Polybrene (Sigma) was added to a final concentration of 8μg/mL to enhance the efficiency of infection. Lentivirus shRNA infections to knockdown BCL9 expression were performed as described previously (19). Briefly, recombinant BCL9 shRNA and control lentiviruses were produced by transient transfection of 293T cells. Colo320 were transduced with virus supernatant containing polybrene, and GFP-expressing cells sorted by FACS.

VEGF ELISA assay

VEGF ELISA was performed as previously described (19). Briefly, cells (1×10^6) were treated with vehicle and SAH-BCL9 peptides (5 μM) for 24 h. VEGF levels in the supernatant were then measured according to the manufacturer's ELISA protocol (DuoSet, R&D Systems).

Protease Resistance of Peptides

Protease reaction samples contained 5 μL peptide in DMSO (1 mM stock) and 195 μL of buffer consisting of 10 mM Tris-HCl buffer pH 7.4 with 1 mM CaCl2 and chymotrypsin (0.5 ng μL). Chymotryptic peptide fragments were analyzed by liquid chromatography/ mass spectrometry (Agilent 1200).

Nuclear/Cytosol Fractionation Kit

2×10^6 cells are performed to separate nuclear extract and cytoplasmic fraction according to protocol of BioVision Nuclear/Cytosol Fractionation Kit, #K266-25.
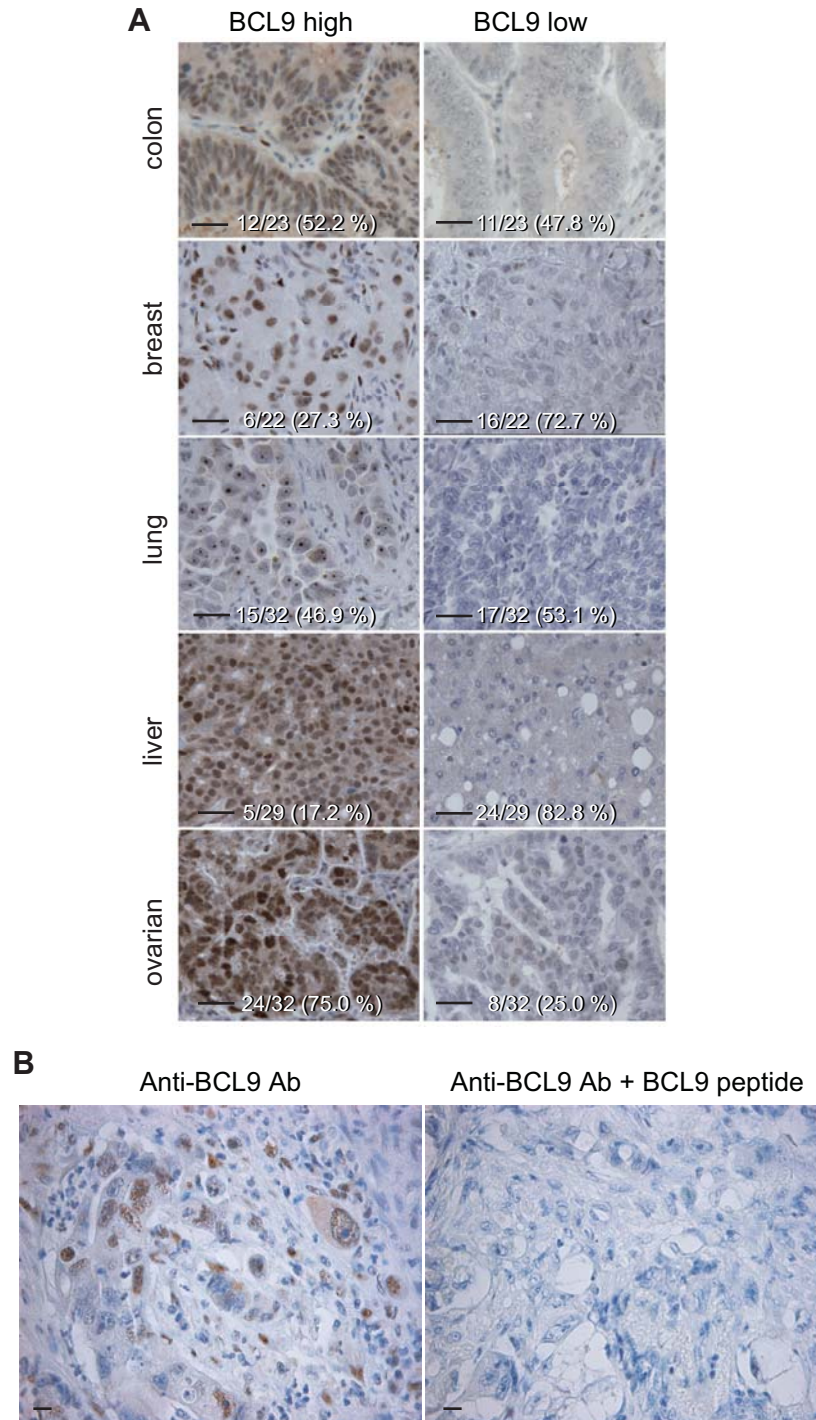
**Fig. S1. BCL9 overexpression in a broad range of human tumor types.**
(A) Immunohistochemical studies performed on tissue microarrays from colon (*n*=23), breast (*n*=22), lung (*n*=32), liver (*n*=29), and ovarian (*n*=32) carcinomas revealed high levels of BCL9 expression in a wide variety of tumors. Representative cases of tumors with high or low level of BCL9 immunostaining are shown. Scale bar: 50μm. (B) Blocking experiments using the immunizing BCL9 peptide (Abcam) were performed on colorectal cancer specimens according to the manufacturer's protocol and documented BCL9 antibody specificity. Scale bar: 50μm.
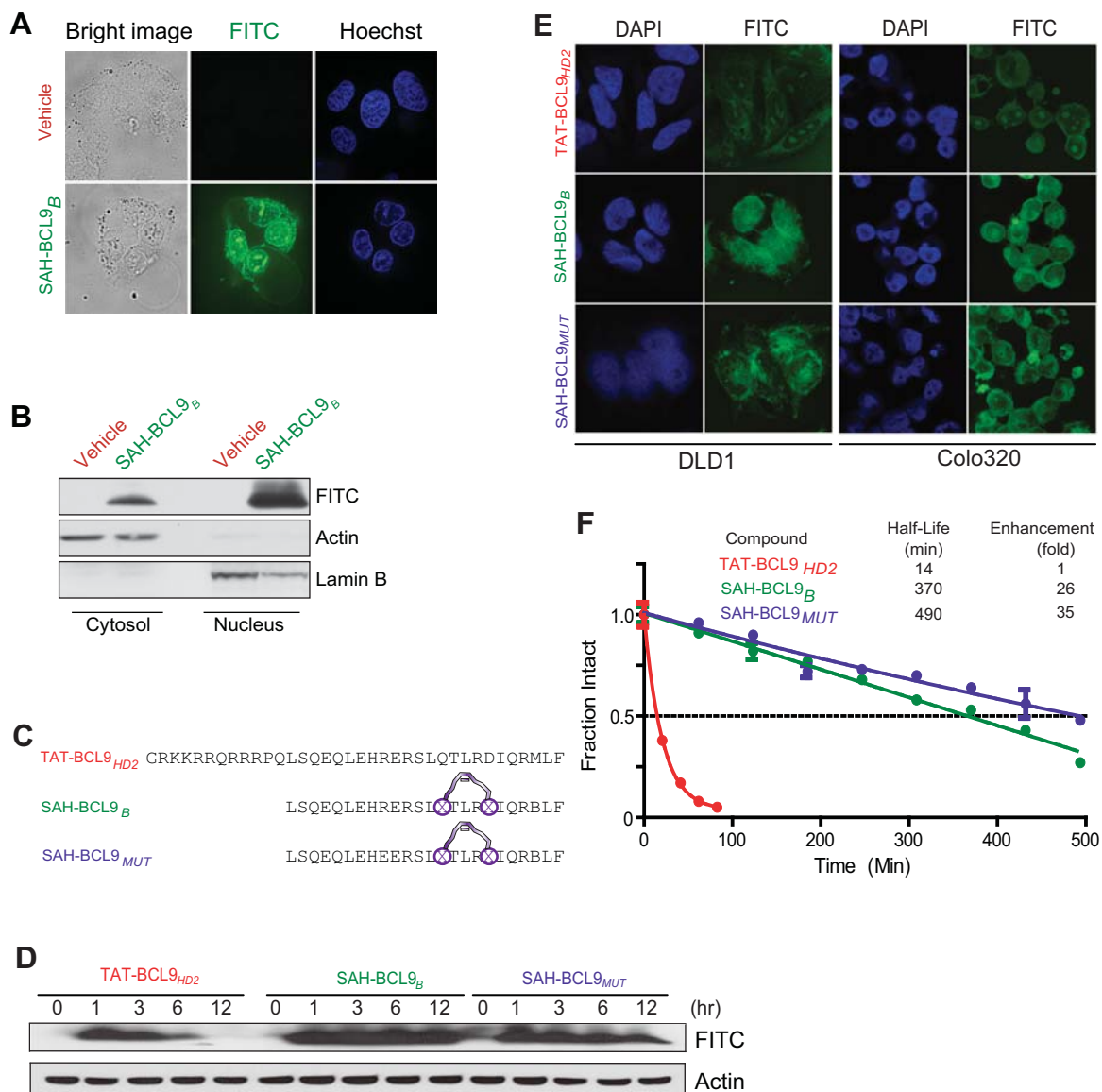
Fig. S2. Cellular uptake and stability of SAH-BCL9$_B$.
Cellular uptake of vehicle and FITC-SAH-BCL9$_B$ was monitored by live cell microscopy **(A)**, and cellular fractionation and immunoblot **(B)** analysis in DLD1 cells. **(C)** Amino acid sequence of TAT-BCL9$_{HD2}$, SAH-BCL9$_B$ and SAH-BCL9$_{MUT}$ peptides. **(D)** Cellular uptake of FITC-TAT-BCL9$_{HD2}$, FITC-SAH-BCL9$_B$ and FITC-SAH-BCL9$_{MUT}$ in Colo320 cells as evaluated by immunoblot analysis of total cell lysates. **(E)** Cellular uptake of FITC-TAT-BCL9$_{HD2}$, FITC-SAH-BCL9$_B$ and FITC-SAH-BCL9$_{MUT}$ peptides in DLD1 (left) and Colo320 (right) cell lines as evaluated by confocal microscopy after 2 hr incubation with 1µm peptide concentration. **(F)** Comparative resistance of FITC-TAT-BCL9$_{HD2}$, FITC-SAH-BCL9$_B$ and FITC-SAH-BCL9$_{MUT}$ peptides to chymotrypsin. Chymotryptic peptide fragments were analyzed by liquid chromatography/mass spectrometry (Agilent 1200).
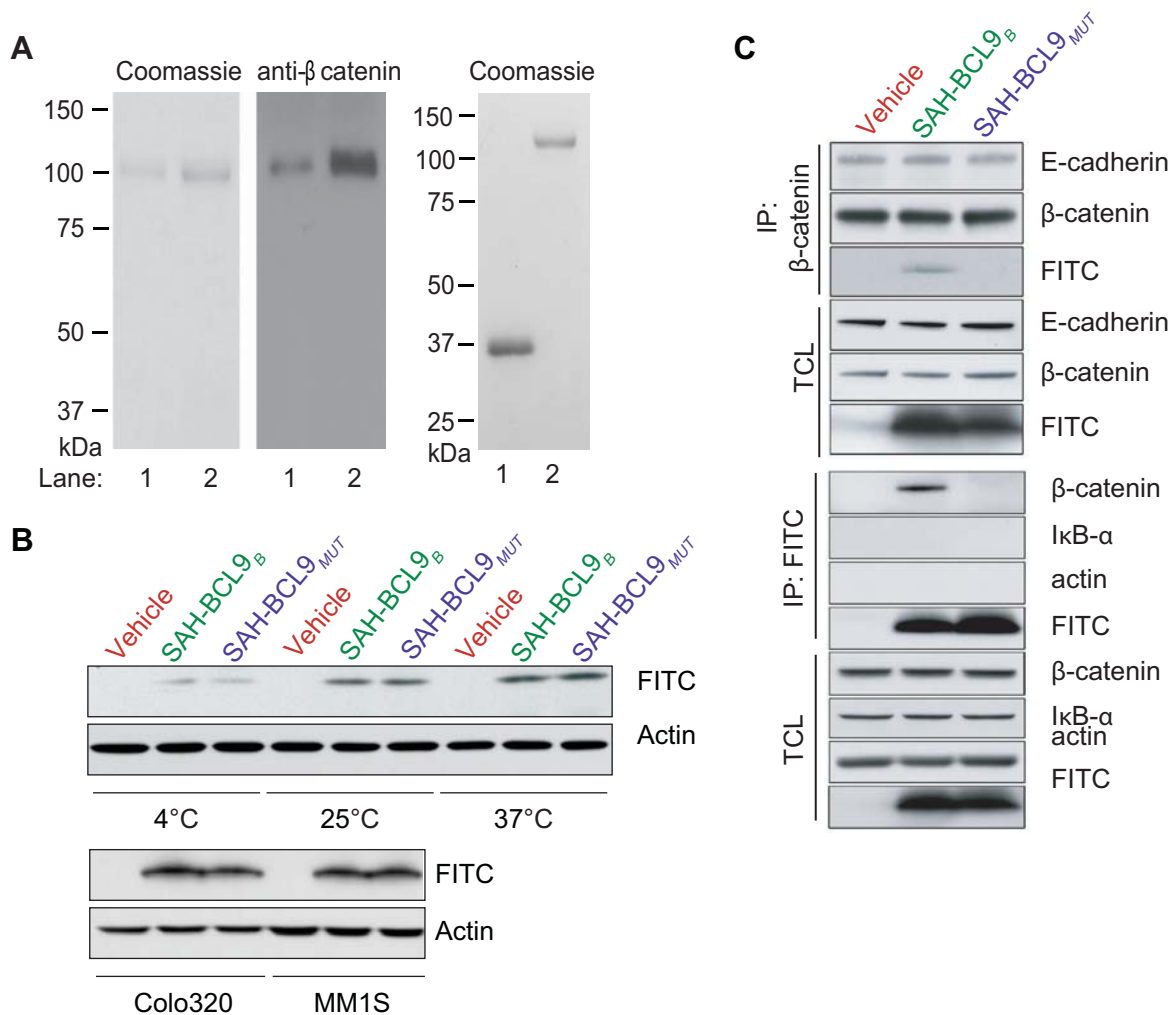
Fig. S3. Selective inhibition of BCL9/β-catenin-driven transcription by SAH-BCL9$_B$.
(A) Full-length GST-tagged hβ-catenin was expressed and then purified to homogeneity, as evaluated by Coomassie staining and anti-β-catenin immunoblot. GST-β-catenin input: Lane 1, 0.2 μg and Lane 2, 0.4 μg (left). His-tagged hBCL9 (residues 243-469) containing the HD2 domain (Lane 1) and full-length GST-tagged hβ-catenin (Lane 2) were produced and purified for use in GST-pull down assays (right). **(B)** FITC-SAH-BCL9$_B$ and FITC-SAH-BCL9$_{MUT}$ peptides exhibit equivalent temperature-dependent uptake in Colo320 cells (top), and cellular uptake in representative colorectal and myeloma cell lines (bottom). **(C)** β-catenin targeting by FITC-SAH-BCL9$_B$ is selective for disruption of the BCL9/β-catenin complex and does not affect anti-β-catenin co-immunoprecipitation of E-cadherin from MCF7 cell lysates (top). Treatment of MCF7 cells with FITC-SAH-BCL9$_B$ followed by anti-FITC pull down performed on cellular lysates revealed the selective interaction between FITC-SAH-BCL9$_B$ and β-catenin, and no co-immunoprecipitation of unrelated proteins such as IκBα and actin (bottom). MCF7 cells were employed in these assays as they contain readily detectable levels of E-cadherin protein for monitoring the β-catenin/E-cadherin interaction. TCL: total cellular lysate.
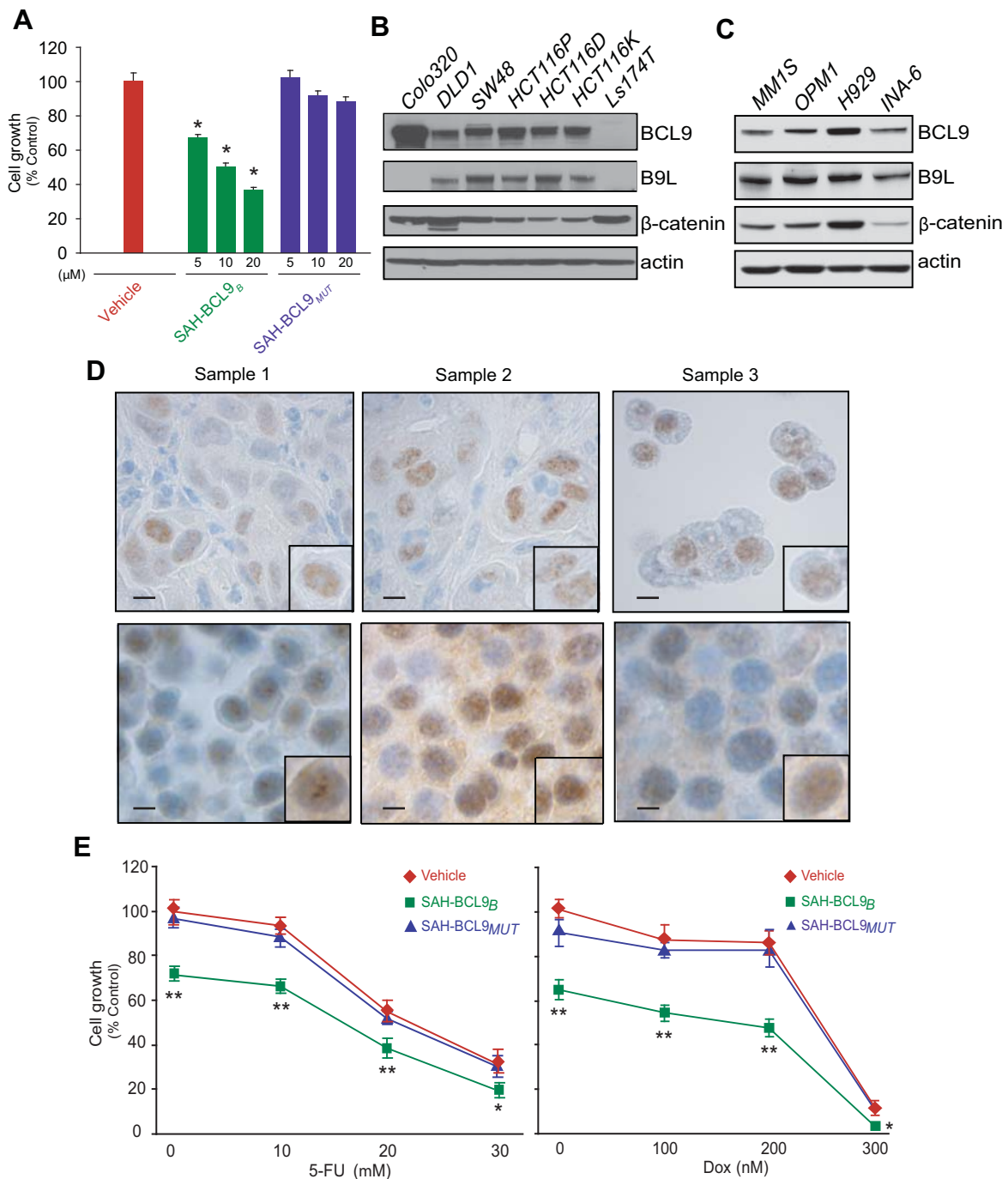
Fig. S4. SAH-BCL9$_B$ enhances the cytotoxic effect of conventional chemotherapeutic agents.

(A) SAH-BCL9$_B$ dose-responsively inhibited the growth of Colo320 cells. *p < 0.01. Expression of BCL9, B9L and β-catenin in CRC **(B)** and MM **(C)** cell lines as evaluated by immunoblot. **(D)** Immunohistochemical analysis of BCL9 expression (brown) in three different cases of CRC (top) and MM (bottom) primary tumors used in the cellular proliferation analyses. Insets highlight expression of BCL9 and its nuclear localization in the tumor cells. Scale bar: 50μm. **(E)** Colo320 (left) and MM1S (right) cells were co-cultured with either vehicle, SAH-BCL9$_B$, or SAH-BCL9$_{MUT}$ and increasing concentrations of 5-flurouracil (5-FU) or doxorubicin (Dox), and evaluated for cellular proliferation using ^{3}H-thymidine incorporation. SAH-BCL9$_B$ but not SAH-BCL9$_{MUT}$ or vehicle significantly enhanced the anti-tumor activity of the conventional agents.
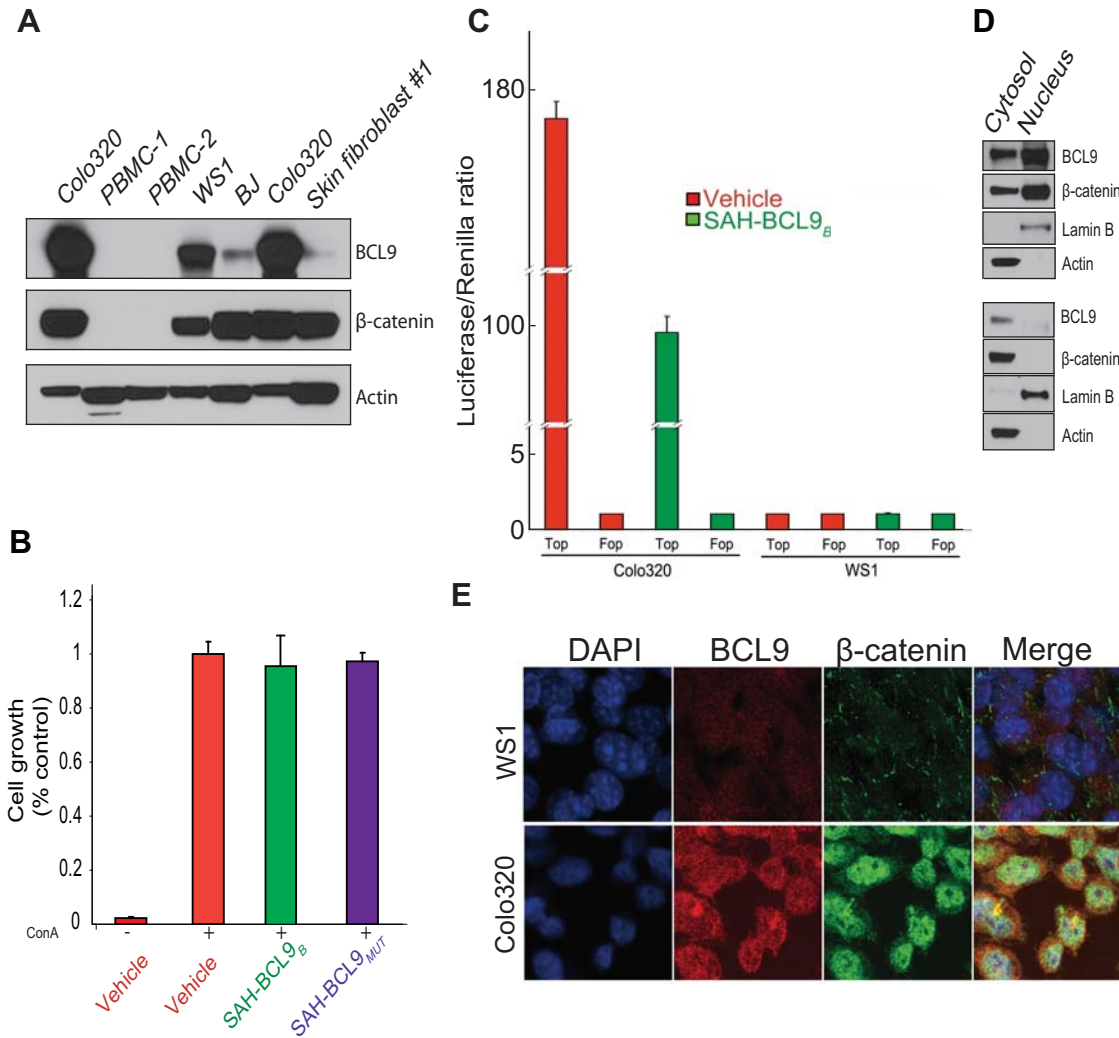
**Fig. S5. Effect of SAH-BCL9$_B$ in non-cancer cells.**
(A) Immunoblot analysis of the expression of BCL9, B9L and β-catenin in normal peripheral blood mononuclear cells (PBMC-1 and PBMC-2), normal skin fibroblasts (WS1 and BJ), and Colo320 cells. **(B)** Effect of SAH-BCL9$_B$ treatment on the growth of PBMC-1 cells as evaluated by [^{3}H]Thymidine incorporation after stimulation with Concanavalin A for 3 days. Error bars are mean +/-s.d. for experiments performed in quadruplicate. **(C)** Colo320 and WS1 cells were transfected with TOP-FLASH and FOP-FLASH, incubated with vehicle (red) or SAH-BCL9$_B$ peptide (10µM), and assayed for luciferase activity, which was normalized to Renilla luciferase control, and TOP-FLASH luciferase activity was normalized to that of FOP-FLASH luciferase activity. Error bars are mean +/- s.d. for assays performed in triplicate. **(D)** Cellular fractionation and immunoblot analyses of BCL9 and β-catenin expression in Colo320 (top) and WS1 (bottom) cells. Lamin B and Actin were used as markers of nuclear and cytoplasmic fractions, respectively. **(E)** Confocal immunofluorescence analysis of BCL9 (red) and β-catenin (green) expression in WS1 (top) and Colo320 (bottom) cells.
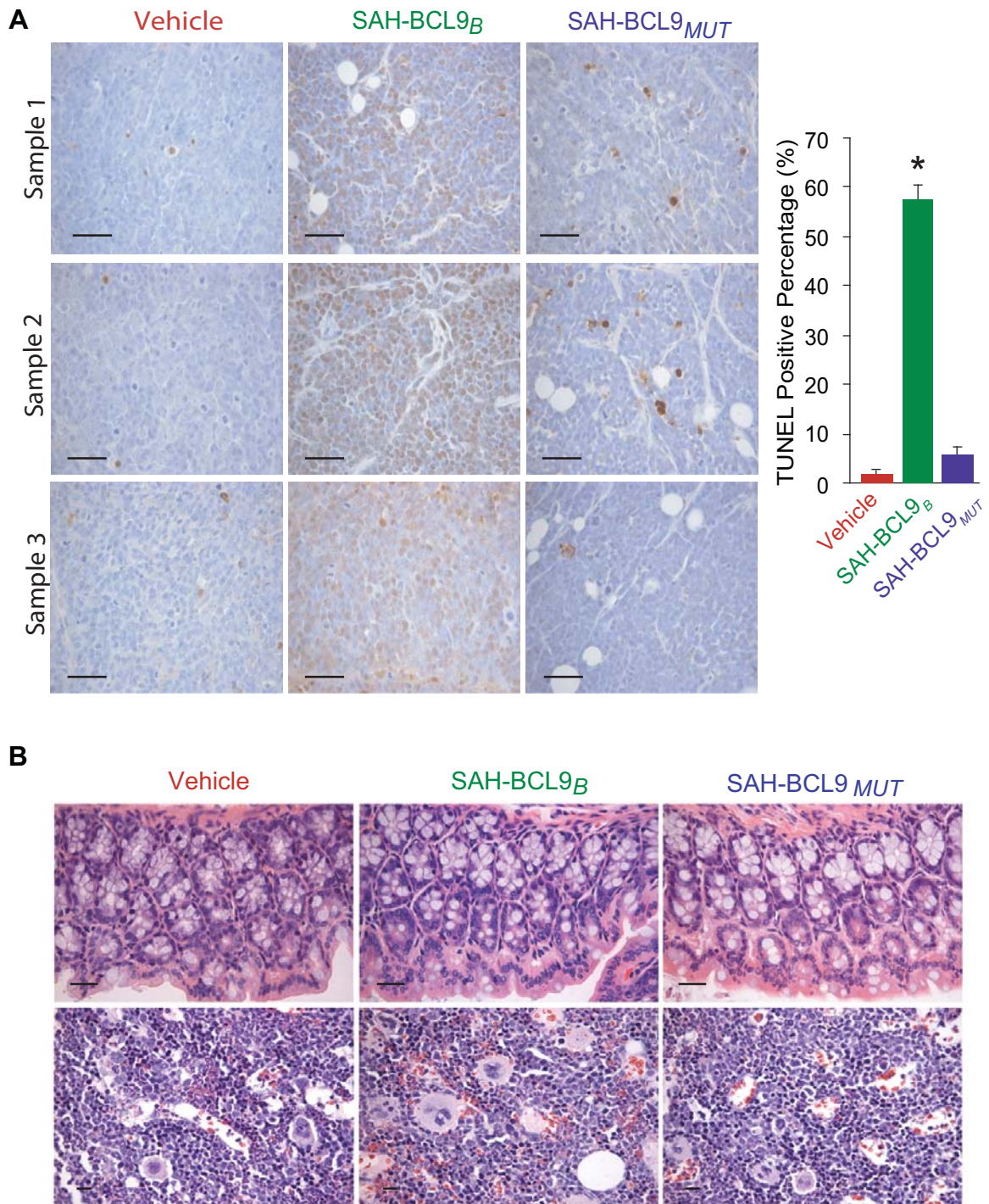
Fig. S6. Histology of tumor tissue, colonic mucosa and bone marrow of SAH-BCL9$_B$-treated mice.
(A) Tumor tissue sections from NOD/SCID mice bearing intraperitoneal Colo320 cells were evaluated for apoptosis induction using the TUNEL assay (brown). SAH-BCL9$_B$, but not vehicle or SAH-BCL9$_{MUT}$, notably increased TUNEL positivity. Three representative 40 X power fields are shown, including quantitation of TUNEL positivity in 3 high power fields. * $p< 0.001$. Scale bar: 50μm. **(B)** H&E staining of colonic mucosa (top) and bone marrow (bottom) tissues isolated from experimental mice injected with colo320 cells and treated with vehicle or SAH-BCL9-peptides showed no evidence of toxicity across all histologic specimens. Scale bar: 125μm.
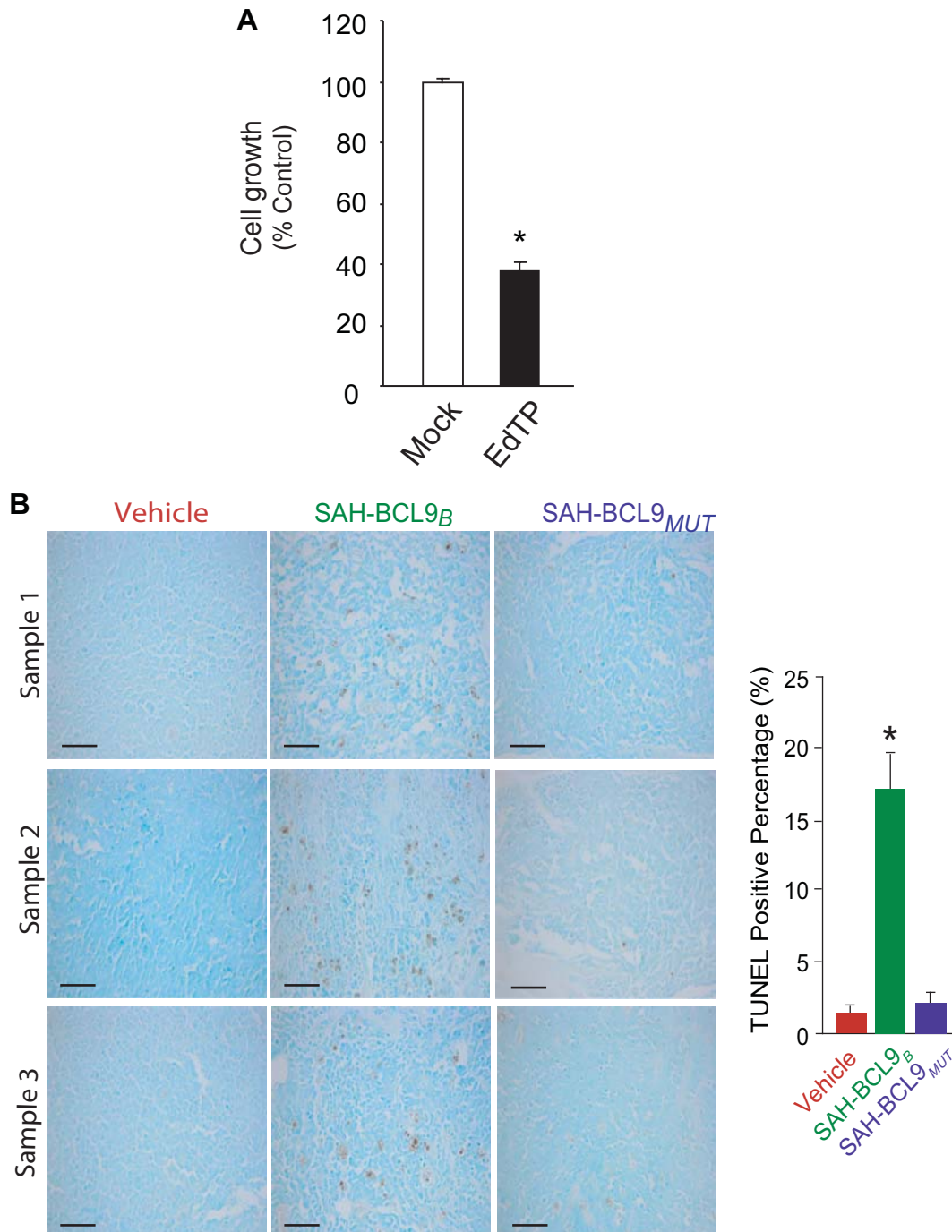
Fig. S7. Proliferation and apoptosis of INA-6 cells.
(A) INA-6 cells were lentivirally transduced with empty vector (Mock) or a vector expressing a dominant negative form of TCF4 (EdTP) and proliferation was measured by ^{3}H-thymidine incorporation. **(B)** Tumor tissue sections from NOD/SCID mice bone chips bearing INA-6 cells were evaluated for apoptosis induction using the TUNEL assay (brown). SAH-BCL9$_B$, but not vehicle or SAH-BCL9$_{MUT}$, notably increased TUNEL positivity. Three representative 40 X power fields are shown, including quantitation of TUNEL positivity in 3 high power fields. * $p < 0.001$. Scale bar: 50μm.
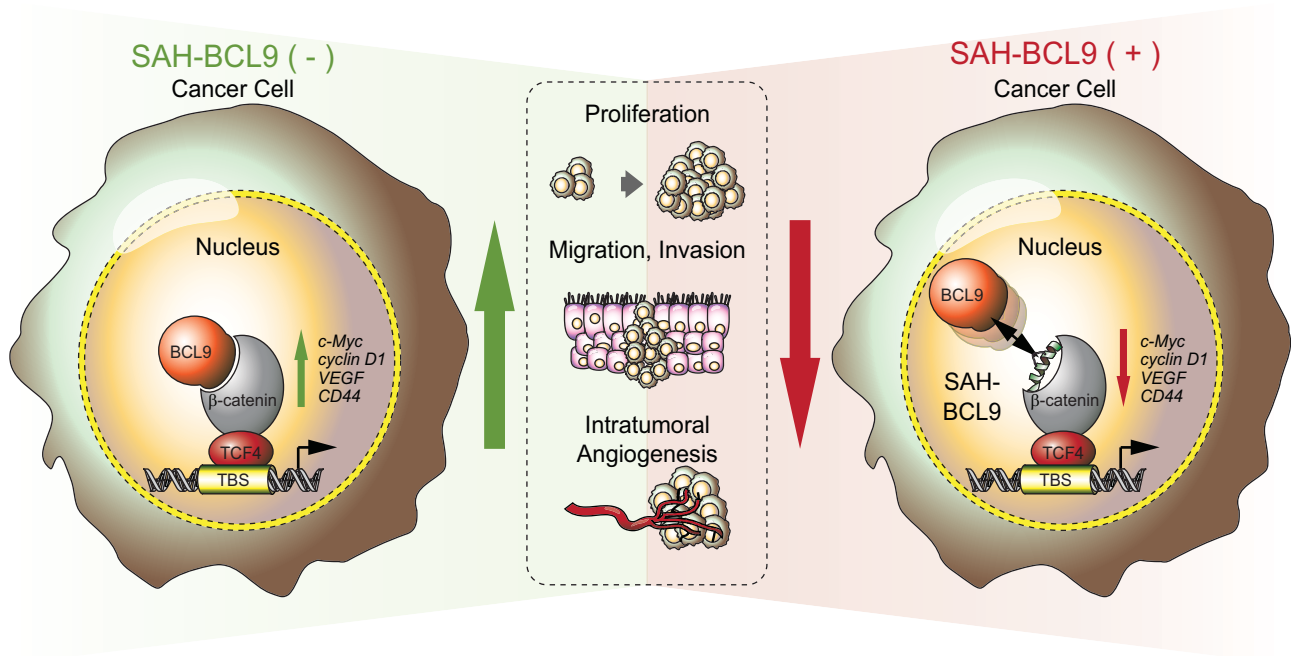
Fig. S8. Wnt transcriptional activity after SAH-BCL9$_B$ treatment.
Deregulated Wnt signaling underlies the pathogenesis of a broad range of human cancers yet the development of targeted therapies to disrupt the pathway has remained a challenge. β-catenin is a central effector of the canonical Wnt pathway, activating the expression of genes such as *c-Myc*, *cyclin D1*, *VEGF*, and *CD44* that are involved in cell proliferation, migration, and angiogenesis. BCL9 is an important co-activator for β-catenin-mediated transcription, and is highly expressed in tumors but not in the cells of origin, presenting an opportunity to selectively inhibit pathologic β-catenin activity. Guided by the structure of the BCL9/β-catenin complex, we generated Stabilized Alpha-Helices of BCL9 (SAH-BCL9) to block Wnt signaling in cancer through targeted disruption of BCL9/B9L/β-catenin complexes. SAH-BCL9 reduces Wnt transcriptional activity and the expression of Wnt/β-catenin transcriptional targets, impeding tumor cell proliferation, migration, invasion, and angiogenesis *in vitro* and *in vivo*. TBS; TCF4 binding site.